Available online at www.sciencedirect.com
SCIENCE DIRECT®
Journal of Solid State Chemistry 177 (2004) 2756–2762
JOURNAL OF SOLID STATE CHEMISTRY
http://elsevier.com/locate/jssc

# Molybdenum nitride fibers or tubes via ammonolysis of polysulfide precursor

Shutao Wang, Zude Zhang,* Yange Zhang, and Yitai Qian

*Department of Chemistry, University of Science and Technology of China, Hefei, Anhui 230026, People's Republic of China*

Received 9 January 2004; received in revised form 6 April 2004; accepted 14 April 2004

**Abstract**

Millimeter-sized molybdenum nitride (MoN), in the forms of fiber-like prisms or hollow tubes, has been successfully synthesized via thermal ammonolysis of molybdenum polysulfide precursor. The initial morphology of the precursor is well preserved in the final product. This method could be expanded to preparation of other fiber-like nonmetal ceramics without addition of template. The polysulfide precursor (abbreviated to PS), hydrothermally prepared at 30°C (PS1) or 150°C (PS2), was characterized by various methods for better comprehension of the sulfide–nitride topotactic conversion model.


*Keywords:* Nitride; Polysulfide; Precursor

## 1. Introduction

Mesoscale materials, a prosperous domain between millimeter and centimeter scale, has generated great interest recently [1–6]. The influence of micro-fabrication technology is also far-reaching [7,8]. Nitrides, with unique physical and chemical properties, have attracted great attentions for their wide applications in many fields [9–14]. Novel synthetic approaches of transition metal nitrides are subjected to intensive studies in the past decades since traditional synthesis entails severe conditions of temperature or pressure. One of the most common routes giving access to nitrides consists of the thermal ammonolysis of oxides [15]. Boudart's group has successfully prepared highly porous transition metal nitrides from oxide platelets [16,17]. Previous work by Herle, Jung and their coworkers, and more recently, by Tessier et al. [18–20], have shown that $Cr_2S_3$, $TiS_2$, $VS_2$, $Al_2S_3$ as well as $WS_2$ all can react with ammonia to give rise to nitrides. $Mo_5N_6$ and $\delta$-MoN has been prepared by ammonolysis of fine reactive $MoS_2$ powders at 750°C and 850°C, respectively [20,21]. In addition, ternary sulfides with stoichiometry of $CuM'_2S_4$ ($M'$ = Ti, Co), $M_xTaS_2$ ($M$ = Cu, Zn, Al, In, Sn), and $MMo_2S_4$ have been used for reaction with ammonia at moderate temperatures to form ternary nitrides [21]. A much more investigated route is the synthesis of sulfides from oxide precursors, following which trioxides can lead to inorganic fullerenes (IF) $MS_2$ ($M$ = Mo, W) [22–26]. Ammonolysis of ternary oxides $FeWO_4$ and $MnMoO_4$ have also been used to synthesize layered ternary nitrides $FeWN_2$ and $MnMoN_2$ [27].

This paper aims at the synthesis of mesoscale mononitride from hydrothermally prepared polysulfide. The initial morphology of the precursor is well preserved in the final product. A precursor based topotactic conversion model can be generalized to more complex systems, even to dimensions on nanoscale.

## 2. Experimental section

### 2.1. Materials preparation

The polysulfide precursors were prepared through the method similar to that described by Müller et al. [28]. An appropriate amount of ammonium heptamolybdate tetrahydrate (AHM; $(NH_4)_6Mo_7O_{24}{\cdot}4H_2O$) and $(NH_4)_2S_x$ were put into a Teflon-lined autoclave

*Corresponding author. Fax: +86-551-360-1592.
*E-mail address:* zzd@ustc.edu.cn (Z. Zhang).

0022-4596/$ - see front matter © 2004 Elsevier Inc. All rights reserved.
doi:10.1016/j.jssc.2004.04.019

(50 mL capacity). The autoclave was then filled with distilled water and maintained at 30°C (PS1) or 150°C (PS2) for 10 h and then allowed to cool to room temperature. The precipitates were separated by filtration, washed sequentially with distilled water, absolute ethanol and carbon bisulfide. After drying in a vacuum at 60°C for 4 h, dark red crystals were collected for further nitridation.

Hexagonal MoN was synthesized by ammonolysis of the above polysulfide precursor through a temperature-programmed reaction (TPR). The polysulfide precursor was placed in a quartz boat inside a quartz tube. Commercial $NH_3$ was introduced into the reactor to expel air before reaction. Then the temperature was raised to 700°C with a heating rate of 10°C $min^{-1}$ under ambient pressure. A thermocouple and a programmed AI-808P Maxonic automatic controller were used to monitor and control temperature. The sample was kept at the final temperature for 5 h. Then the furnace was switched off and the sample was naturally cooled to room temperature in flowing $NH_3$. Nitrides resulting from PS1 and PS2 are labeled MoN1 and MoN2, respectively.

### 2.2. Materials characterization

Crystallographic information of nitride samples, including the sulfide precursor, was investigated with X-ray powder diffraction (XRD) on a Philips X'Pert Pro Super diffractometer. Diffraction data were collected over the $2\theta$ range from 10° to 70°. Fourier transform infrared (FT-IR) spectra were recorded using pressed KBr disks with a Bruker EQUINOX55 apparatus. The morphology of the precursor was examined before and after nitridation reactions with scanning electron microscopy (SEM) using a HITACHI X-650 microscope. X-ray photoelectron spectroscopy (XPS) was recorded on a VG ESCALAB MK II spectrometer to measure elemental composition of the sample. The binding energies (BE) obtained in XPS analysis were corrected by referencing the C 1*s* line to 284.60 eV.

## 3. Results and discussion

Fig. 1a compares the XRD patterns of precursor PS1 and PS2. Both of them are indexed as monoclinic $(NH_4)_2[Mo_3(S_2)6S] \cdot H_2O$ (JCPDS Card No. 762038). Obtained under hydrothermal conditions at different temperature, the precursors show different growth planes, which would possibly leads to diverse reactivity with ammonia. XRD patterns of corresponding nitrides are shown in Fig. 1b. MoN1 is indexed as mixtures of hexagonal molybdenum nitride (JCPDS Card No. 771999) and intermediate sulfide ($Mo_6S_{9.5}$, JCPDS Card No. 411328), while ammonolysis of PS2 leads to

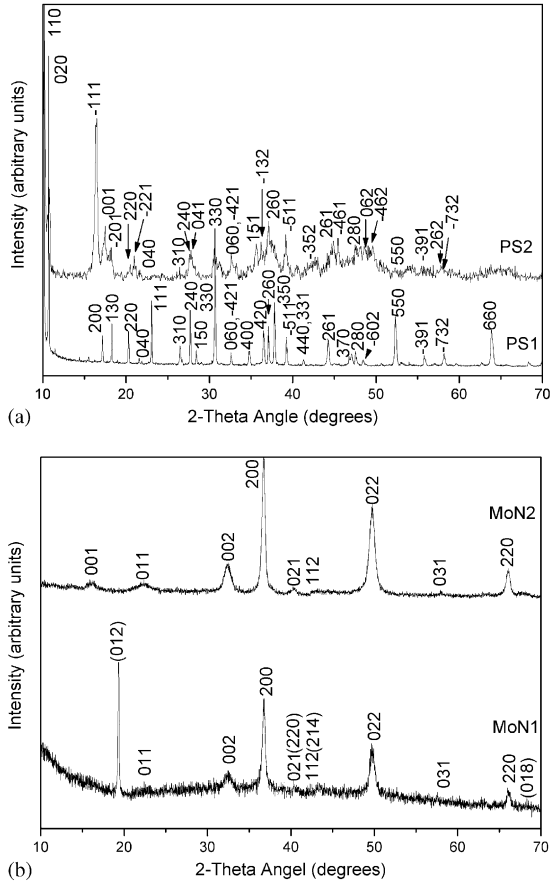


Fig. 1. XRD patterns of precursors and nitrides via ammonolysis at 700°C for 5 h. (a) Precursors: PS1 and PS2 are both indexed as monoclinic $(NH_4)_2[Mo_3(S_2)6S] \cdot H_2O$ (JCPDS Card No. 762038). (b) Nitrides: MoN1 is indexed as a mixture of hexagonal MoN (JCPDS Card No. 771999) and $Mo_6S_{9.5}$ (JCPDS Card No. 411328; indexes put in parenthesis). MoN2 is indexed as hexagonal MoN (JCPDS Card No. 771999).

mononitride in pure phase. Nitridation of PS2 appears much easier and faster compared with PS1, which could be attributed to different temperature at which the precursor was produced. The higher diffraction intensities of (200) plane relative to other planes of nitride implies there are preferential orientation parallel to the (100) plane, which is generally the consequence of topotactic transformation from highly anisotropic precursors. The peak broadening of (002), (022) and (220) plane reflects abundant defects or aberrations occur in the nitride crystals. These defects are expected to run parallel with (100) plane, the diffraction peak width of which will otherwise also be broadened. A series of samples were synthesized from PS2 at temperatures of 600°C, 650°C, 700°C and 750°C, respectively to find out more about the details of the reaction (Fig. 2). It has been found that $MoS_2$ is the intermediate at relative low reaction temperature.

Fig. 3 shows the FT-IR spectra of precursor PS2 and nitride MoN2. The IR spectra are assigned according to

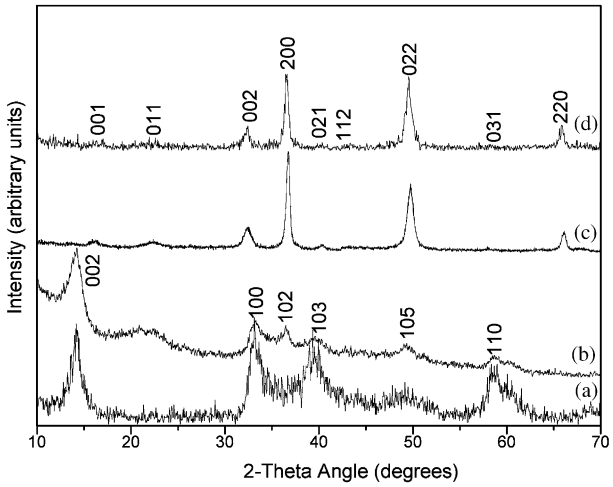


Fig. 2. XRD patterns of samples prepared from PS2. (a) via ammonolysis at 600°C for 5 h, indexed as $MoS_2$ (JCPDS Card No. 751539). (b) Via ammonolysis at 650°C for 5 h, indexed as $MoS_2$ (JCPDS Card No. 751539). (c) Via ammonolysis at 700°C for 5 h, indexed as MoN (JCPDS Card No. 771999). (d) Via ammonolysis at 750°C for 5 h, indexed as MoN (JCPDS Card No. 771999).

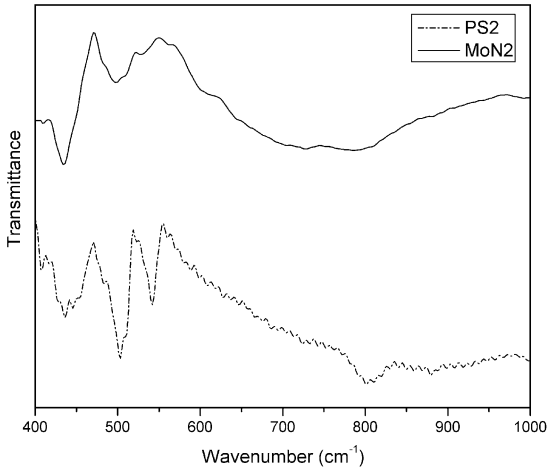


Fig. 3. FT-IR spectra of precursor PS2 and nitride MoN2.

literature reports (Table 1) [8,9,23]. For PS2, the band around 542 and 503 $cm^{-1}$ are assigned to stretch vibrations of bridging sulfur $(S–S)_{br}$ and terminal sulfur $(S–S)_{ter}$, respectively. Signals between 400 and 440 $cm^{-1}$ are characteristic of Mo–S–Mo vibrations. For MoN, the broadband between 750 and 1000 $cm^{-1}$, and the band below 700 $cm^{-1}$ reflect the ν(Mo–O) stretch vibrations resulting from surface oxidation. Possible existence of residual Mo–O bonds in PS2 could not be excluded since the IR peaks of PS2 have significant overlap with the Mo–O impurity peaks from MoN2, yet it is believed that the amount of Mo–O bonds is very small and can be omitted since they could not be detected by the XRD patterns.

Table 1
Assignment of IR spectra

| PS2 | | MoN2 | |
|---|---|---|---|
| ($cm^{-1}$) | Assignment | ($cm^{-1}$) | Assignment |
| 408 | Mo–S | 435 | Mo–O |
| 436 | Mo–S | 498 | Mo–O |
| 503 | Mo–S, $(S–S)_{ter}$[a] | 534 | Mo–O |
| 542 | $(S–S)_{br}$[b] | 688 | Mo–N |
| 801 | Mo–O | 786 | Mo–O |

[a] $(S–S)_{ter}$ denotes terminal sulfur.
[b] $(S–S)_{br}$ denotes bridging sulfur.

The principle of synthesis is based on a gas–solid reaction. Pseudomorphy generally occurs in systems containing gas and solid precursors [15]. As revealed by the SEM micrographs in Fig. 4, nitride is pseudomorphous with polysulfide precursor in this experiment. There are two types of characteristic morphologies, straight fiber-like or tube-like prism structure, in the precursors and final nitrides. Morphology and size distribution of the nitrides bears close resemblance to that of the polysulfide precursors. The crystal morphology was finally determined by the rate of anisotropic growth if the ratio of growth rate of each crystal face keeps constant. According to the law of Bravais, {100} planes will dominate in the surface of nitrides with hexagonal symmetry. Scheme 1 shows a projection of a nitride crystalline with a typical unsymmetrical hexagonal cross-section along the [001] direction. Details about morphology observation of SEM micrographs are shown in Table 2. Though original size and shape of the precursor are almost unchanged, the width of facets and the length of the fiber-like or tube-like prisms are slightly reduced after nitridation treatment. Similar observation has also been obtained for the sulfidation of α-$MoO_3$ nanorods, owing to lattice parameter variations [29]. The cross-sections of all the fibers or tubes are irregularly asymmetric polygons instead of symmetric circles. A close-up view (Fig. 4d) shows the inside surface of the tubes exhibits a great diversity of textures and geometries. The reason for this phenomenon is unclear. It is remarkable that the precursor (Fig. 4a) appears to be smooth and dense, while the nitride is somewhat brittle with some cracks and even splits, as shown in Figs. 4b and c. These microcraks are induced by stress. Thermal expansion or shrinkage, considerably anisotropic along the axis of *a*, *b*, and *c*, are believed to be a stress raiser. Stress inside the samples may also results from change of cell parameters and uneven distribution of components during the process of ammonolysis. As a result, microcracks and even ruptures shall emerge when the cumulative stress exceeds a critical value [15,30,31]. It is possible that compact samples can be obtained with certain additives

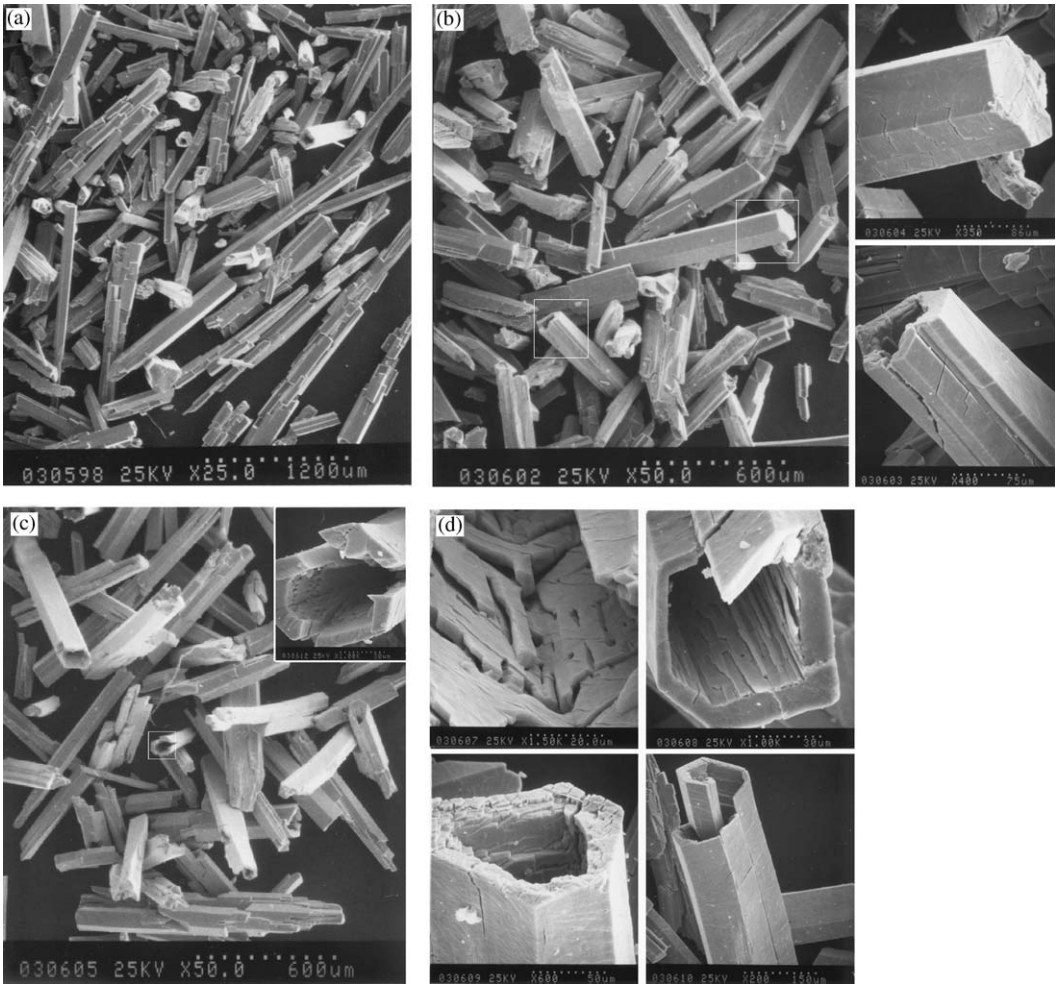


Fig. 4. SEM micrographs of precursor and corresponding nitride. (a) Precursor PS2; (b) intermediate via ammonolysis of precursor PS2 at 600°C for 5 h. Insets are magnified images of the framed parts, showing typically a fiber and a tube with microcracks; (c) nitride MoN2. Inset is a magnified image of the framed part, where obvious ruptures occur; and (d) examples of various textures and geometries of the inside surface and end cross-sections of nitride tubes.

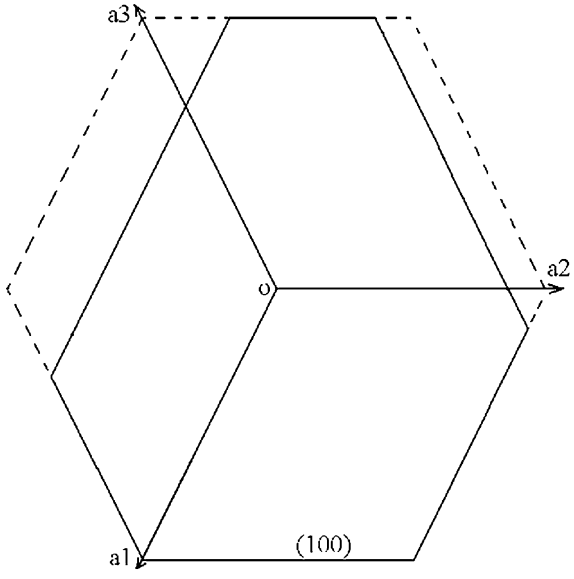


Scheme 1. Projection of a nitride crystalline along [001] direction with a typical unsymmetrical hexagonal cross-section.

[32]. Ammonia has been reported to be a unique reactant to drive the solid transformation into a topotactic route. Simultaneously nitridation and reduction of the starting material is a key point leading to topotactic route, which is often characterized by the effect of pseudomorphy. Combined with XRD results, it is confirmed topotactic relationship does occur between polysulfide precursors and nitrides [33].

The ammonolysis mechanism is proposed to be mass-diffusion controlled [24,29,34], similar to conversion from oxide to sulfide. Since the precursor was fully exposed to an atmosphere of ammonia, which could reacts equally with all the active sites at the surface of the precursor, the nitridation process starts most likely at the surface of the precursor and then propagates inwards instead of progression of the nitride front and depletion of the sulfide from one end to the other. Ammonia was chemisorbed firstly onto the surface of precursor, with unpaired electrons of nitrogen donated to the unfilled *d* orbits of molybdenum. On the other

Table 2
Details about morphology observation of SEM micrographs

| Sample | Width of facets in fiberlike prisms (ìm) | Width of facets in tubelike prisms (μm) | Length (mm) |
|---|---|---|---|
| PS2 (Fig. 4a) | 65–130 | 65–130 | 0.39–1.95 |
| Intermediate (Fig. 4b)[a] | 32–113 | 32–84 | 0.24–0.81 |
| MoN2 (Fig. 4c) | 48–81 | 32–97 | 0.28–0.81 |

[a] Prepared via ammonolysis of PS2 at 600°C for 5 h.

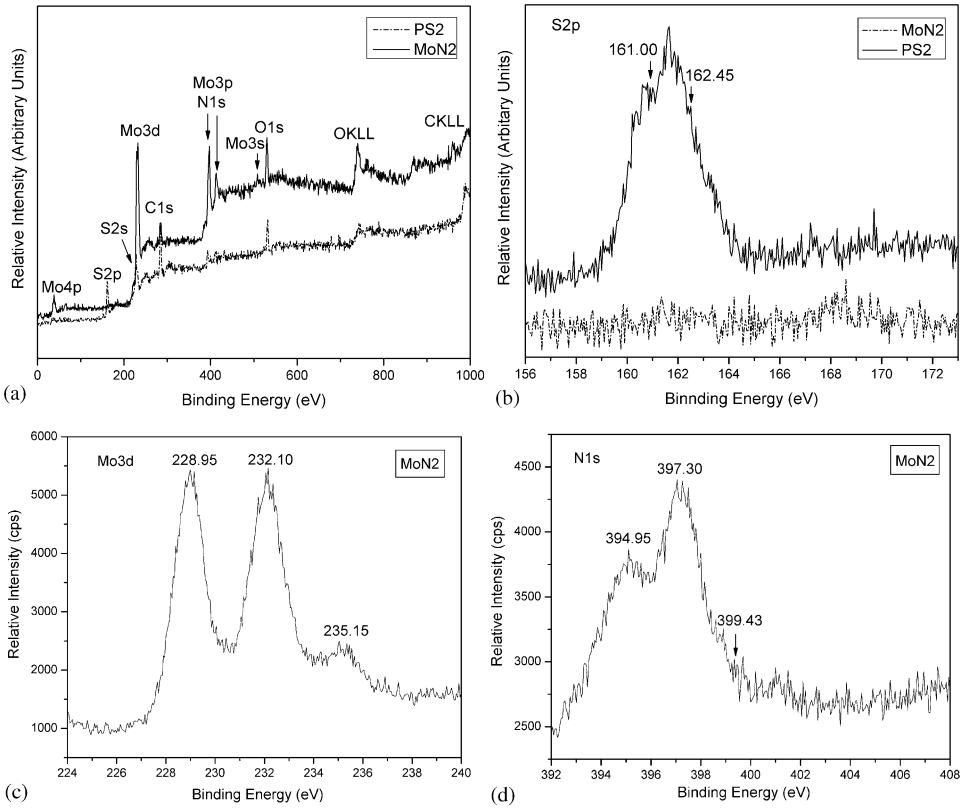


Fig. 5. XPS spectra of precursor PS2 and nitride MoN2. (a) survey spectra; (b) high resolution spectra of S 2*p*; (c) high resolution spectra of Mo 3*d*; (d) high resolution spectra of N 1*s*.

hand, the electronegativity of nitrogen (3.04) is stronger than that of sulfur (2.58) [35]. Therefore, the adsorbed nitrogen outvie sulfur to bond more effectively with molybdenum. Gradually sulfur was replaced from the precursor, broken of Mo–S bond and formation of Mo–N bond occurs simultaneously, accompanying inward diffusion of ammonia. The coordination polyhedron of the Mo atom is a distorted dodecahedron (D2d) with one missing ligand [28]. Terminal $S_2^{2-}$ groups may undergo a ligand exchange reaction with ammonia while elimination of bridging sulfur as $H_2S$ gas may induce defects, both in turn facilitate ammonia adsorption and inward diffusion [21]. Thus the nitridation can reach the core of those solid fibers, different from the sulfidation of molybdenum oxides, where only the top surface of the oxides reacts [22]. As a result, the initial morphology of polysulfide precursor is well-retained through this in situ ammonolysis reaction, as visualized from the SEM morphology micrographs.

Tenne et al. have reported that size distribution of the IF particles is determined by that of the incipient oxide particles [22,25,36]. Previous studies of the reaction of $MoO_3$ with ammonia by Boudart et al. showed that the final product may retain the particle morphology of the starting material [37]. Morphological analogy between $Mo_5N_6$ powder and its $MoS_2$ precursor has also been observed [21]. Similar trends have been observed likewise as to the conversion of WC to $WS_2$ [38]. Synthesis of $WS_2$ nanotubes starting from long $WO_{3-x}$ nanowhiskers is also reported elsewhere [34]. The precursor plays a role of a reactive structural framework in the experiment of this paper, as well as those reported in the above literature. An oxide–sulfide conversion model was proposed by Tenne's group to account for the formation

of IF [22,39]. Similarly, a sulfide–nitride topotactic conversion model can be deduced here to justify the formation of fiber-like or tube-like molybdenum nitrides.

All the samples were thoroughly crushed with a pestle in a mortar before XPS measurement to ensure that information from fresh cross-sections will also be detected and thus represent status of both the surface and the interior of the samples. The XPS survey spectra (Fig. 5a) shows that there are no other impurities in the nitride. Nitrogen peak emerged while sulfur peak of PS2 disappeared in the final product MoN2. For PS2, the BE of S $2p_{3/2}$ at 161.00 eV and 162.45 eV can be assigned to $(S–S)_{ter}$ and $(S–S)_{br}$ in the $Mo_3S_{13}^{2-}$ cluster, respectively (Fig. 5b) [23,28]. The elimination of $(S–S)_{br}$ is supposed to be more difficult since its BE is higher that that of $(S–S)_{ter}$, owing to the presence of Mo–S bond. For MoN2, there is no characteristic S peak occurs (Fig. 5b), indicating complete conversion of polysulfide precursor. Fig. 5c exhibits that Mo core is spin–orbit split to $3d_{5/2}$ (228.95 eV) and $3d_{3/2}$ (232.10 eV), which could be attributed to Mo (III). The BE at 235.15 eV can be ascribed to aerial oxidation of the surface. In Fig. 5d, the N 1*s* peak at 397.30 eV is close to that of N 1*s* in TiN (397.2 eV) [10], suggesting formation of Mo–N bond. The BE around 400 eV is caused by $NH_x$ surface groups for $NH_3$ unlikely exists in the high vacuum conditions for XPS analysis. The shoulder peak at 394.95 eV can be attributed to BE of Mo 3*p*. It is noteworthy that the BE signal of Mo 3*p* and N 1*s* overlaps, and that of Mo 3d and S 2*s* overlaps too [8,40]. Furthermore, surface oxidation had occurred, so this analysis is only qualitative in nature.

## 4. Conclusions

Hydrothermally prepared polysulfide has been converted to millimeter-sized MoN fibers or tubes via ammonolysis at 700°C for 5 h. The morphology of nitride is closely related to that of the starting polysulfide. The current process, where no template removal or subsequent purification is required, provides a new method to explore large three-dimensional (3D) materials. Sulfide–nitride topotactic conversion model is proposed based on previous oxide–sulfide conversion model. This model is expected to be applied to analogical systems on mesoscale or even nanoscale.

## Acknowledgments

We gratefully acknowledge the financial support from the National Natural Science Research Foundation of China.

## References

[1] A. Terfort, N. Bowden, G.M. Whitesides, Nature 386 (1997) 162–164.
[2] J. Tien, T.L. Breen, G.M. Whitesides, J. Am. Chem. Soc. 120 (1998) 12670–12671.
[3] T.L. Breen, J. Tien, S.R.J. Oliver, T. Hadzic, G.M. Whitesides, Science 284 (1999) 948–951.
[4] J.Q. Hu, B. Deng, Q.Y. Lu, K.B. Tang, R.R. Jiang, Y.T. Qian, G.E. Zhou, A. Cheng, Chem. Commun. (2000) 715–716.
[5] K.D. Hermanson, S.O. Lumsdon, J.P. Williams, E.W. Kaler, O.D. Velev, Science 294 (2001) 1082–1086.
[6] V.R. Thalladi, A. Schwartz, J.N. Phend, J.W. Hutchinson, G.M. Whitesides, J. Am. Chem. Soc. 124 (2002) 9912–9917.
[7] W.P. Hoffman, H.T. Phan, P.G. Wapner, Mater. Res. Innov. 2 (1998) 87–96.
[8] P. Afanasiev, C. Geantet, C. Thomazeau, B. Jouget, Chem. Commun. (2000) 1001–1002.
[9] B. Vaidhyanathan, D.K. Agrawal, R. Roy, J. Mater. Res. 15 (2000) 974–981.
[10] L.E. Griffiths, M.R. Lee, A.R. Mount, H. Kondoh, T. Ohta, C.R. Pulham, Chem. Commun. (2001) 579–580.
[11] I.P. Parkin, Chem. Soc. Rev. 25 (1996) 199–207.
[12] W.Q. Han, S.S. Fan, Q.Q. Li, Y.D. Hu, Science 277 (1997) 1287–1289.
[13] E.G. Gillan, R.B. Kaner, Inorg. Chem. 33 (1994) 5693–5700.
[14] Y. Zhang, K. Suenaga, C. Colliex, S. Iijima, Science 281 (1998) 973–975.
[15] C.H. Jaggers, J.N. Michaels, A.M. Stacy, Chem. Mater. 2 (1990) 150–157.
[16] S.T. Oyama, Catal. Today 15 (1992) 179–200.
[17] L. Volpe, M. Boudart, Catal. Rev. Sci. Eng. 27 (1985) 515.
[18] P.S. Herle, M.S. Hegde, N.Y. Vasathacharya, S. Philip, J. Solid State Chem. 134 (1997) 120–127.
[19] W.-S. Jung, S.-K. Ahn, Mater. Lett. 43 (2000) 53–56.
[20] F. Tessier, R. Marchand, J. Alloy Compound 262–263 (1997) 410–415.
[21] R. Marchand, F. Tessier, F.J. DiSalvo, J. Mater. Chem. 9 (1999) 297–304.
[22] Y. Feldman, G.L. Frey, M. Homyonfer, V. Lyakhovitskaya, L. Margulis, H. Cohen, G. Hodes, J.L. Hutchison, R. Tenne, J. Am. Chem. Soc. 118 (1996) 5362–5367.
[23] Th. Weber, J.C. Muijsers, J.H.M.C. van Wolput, C.P.J. Verhagen, J.W. Niemantsverdriet, J. Phys. Chem. 100 (1996) 14144–14150.
[24] A. Rothschild, G.L. Frey, M. Homyonfer, R. Tenne, M. Rappaport, Mater. Res. Innov. 3 (1999) 145–149.
[25] J. Sloan, J.L. Hutchison, R. Tenne, Y. Feldman, T. Tsirlina, M. Homyonfer, J. Solid State Chem. 144 (1999) 100–117.
[26] M. Hershfinkel, L.A. Gheber, V. Volterra, J.L. Hutchison, L. Margulis, R. Tenne, J. Am. Chem. Soc. 116 (1994) 1914–1917.
[27] D.S. Bem, C.M. Lampe-Önnerud, H.P. Olsen, H.-C. zur loye, Inorg. Chem. 35 (1996) 581–585.
[28] A. Müller, V. Wittneben, E. Krickemeyer, H. Bögge, M. Lemke, Z. Anorg. Allg. Chem. 605 (1991) 175–188.
[29] X.W. Lou, H.C. Zeng, Chem. Mater. 14 (2002) 4781–4789.
[30] R.P. Lowell, P. Vancappellen, L.N. Germanovich, Science 260 (1993) 192–194.
[31] V. Korthuis, N. Khosrovani, A.W. Sleight, N. Roberts, R. Dupree, W.W. Warren, Chem. Mater. 7 (1995) 412–417.
[32] J.W. Cao, A. Okada, N. Hirosaki, J. Eur. Ceram. Soc. 22 (2002) 237–245.
[33] S. Li, W.B. Kim, J.S. Lee, Chem. Mater. 10 (1998) 1853–1862.
[34] A. Rothschild, J. Sloan, R. Tenne, J. Am. Chem. Soc. 122 (2000) 5169–5179.

[35] J.A. Dean, Lange's Handbook of Chemistry, McGraw-Hill, Inc., New York, 1999, p. 4–29.
[36] M. Homyonfer, B. Alperson, Y. Rosenberg, L. Sapir, S.R. Cohen, G. Hodes, R. Tenne, J. Am. Chem. Soc. 119 (1997) 2693–2698.
[37] L. Volpe, M. Boudart, J. Solid State Chem. 59 (1985) 332–347.
[38] A. Rothschild, J. Sloan, A.P.E. York, M.L.H. Green, J.L. Hutchison, R. Tenne, Chem. Commun. (1999) 363–364.
[39] A. Zak, Y. Feldman, V. Alperovich, R. Rosentsveig, R. Tenne, J. Am. Chem. Soc. 122 (2000) 11108–11116.
[40] P. Afanasiev, G.-F. Xia, G. Berhault, B. Jouguet, M. Lacroix, Chem. Mater. 11 (1999) 3216–3219.